*Наносистеми, наноматеріали, нанотехнології*
*Nanosistemi, Nanomateriali, Nanotehnologii*
2024, т. 22, № 3, сс. 623–636
https://doi.org/10.15407/nnn.22.03.623



PACS numbers: 73.61.-r, 77.22.Ch, 77.22.Gm, 78.66.Li, 78.67.Sc, 81.15.Cd, 81.40.Tv

# Study of the Effect of Li Doping on ZnO Films Using RF-Magnetron Sputtering Method at Low Temperature

Israa Akram Abbas, Ameera J. Kadhm, and Raheem Lafta Ali

*College of Education for Pure Science,*
*Department of Physics,*
*Al-Mustansiriyah University,*
*Baghdad, Iraq*

In this study, we investigate the effect of Li-doping concentrations (3, 6, and 9%) on the optical and electrical properties of Li-doped ZnO-containing films. Li-doped ZnO films are fabricated by the RF-magnetron sputtering process. The optical and electrical properties of thin-film deposition at different sputtering RF powers in the plasma chamber are investigated. The electrical and optical properties of the thin layer are studied. The results for the optical properties of thin films (ZnO/Li) show that the absorbance, absorption coefficient, and optical conductivity increase with increasing Li concentration, while the energy band gap and transmittance decrease with increasing Li concentration. For all tested temperatures, the D.C. conductivity of the ZnO film increases after Li doping. The D.C. test shows that all films have the same activation energy, and the value of this energy increases as the Li-doping ratio increases. The electrical properties of alternating current demonstrate that, as the frequency of the electric field increases, the dielectric constant and dielectric loss of all films decrease.

У цьому дослідженні ми вивчаємо вплив концентрацій леґувального Літію (3, 6 і 9%) на оптичні й електричні властивості плівок, що містять ZnO, леґованих Літієм. Плівки ZnO, леґовані Літієм, було виготовлено методом радіочастотного (РЧ) магнетронного розпорошення. Досліджено оптичні й електричні властивості осадження тонких плівок за різних потужностей РЧ-розпорошення у плазмовій камері. Досліджено електричні й оптичні властивості тонкого шару. Результати стосовно оптичних властивостей тонких плівок (ZnO/Li) показують, що поглинання, коефіцієнт поглинання й оптична провідність зростають зі збільшенням концентрації Li, тоді як ширина забороненої зони та коефіцієнт пропускання зменшуються зі збільшенням концентрації Li. Для всіх протестованих температур провідність на постійному струмі плівки ZnO збільшується після леґування Li. Тест стосовно постійного струму показує, що всі плівки мають однакову енергію активації, а значення цієї енергії зростає зі збільшенням рівня леґування Літієм. Електричні властивості стосовно змінного струму показують, що зі збільшенням частоти електричного поля діелектрична проникність і діелектричні втрати всіх плівок зменшуються.

**Key words:** ZnO films, RF-magnetron sputtering method, Li doping, nanocomposite, optical and electrical properties.

**Ключові слова:** плівки ZnO, метод радіочастотного магнетронного розпорошення, леґування Літієм, нанокомпозит, оптичні й електричні властивості.

*(Received 4 September, 2023; in revised form, 5 January, 2024)*

## 1. INTRODUCTION

The numerous commercial applications of ZnO nanostructures in medication, colorants, catalysts, ceramics, and elastic-added substances have made it one of the most promising oxide materials. ZnO nanostructures have the potential to be utilized in sun-powered cells, anodes, sensors, straightforward UV defensive coatings, UV outflow, surface acoustic waves, and magnetooptical frameworks [1–8]. In any case, to create ZnO-based optoelectronic gadgets, the fabric must be doped to get *n*-type and *p*-type. Common ZnO shows *n*-type conductivity due to rotating zinc or oxygen openings, as is broadly known.

Nevertheless, it is troublesome to get steady *p*-type ZnO, primarily since the acceptor can compensate for characteristic absconds [9, 10]. Another issue that limits *p*-type conduction in ZnO is the nearness of remaining pollutants at noteworthy donor-like concentrations [11].

To date, a number of reports [12–19] have been distributed on *p*-type Li-doped ZnO lean movies manufactured by different strategies and explored the impact of arrangement conditions such as temperature and post-incubation concentrations lean layer motion picture resource. In any case, to our knowledge, some papers on Li-doped ZnO sol–gel lean movies with *p*-type nanostructures have been distributed [18, 19]. It has been specified that *p*-type conduction can happen when the Li concentration is greater than or breaks even at 10%.

In this study, we examine the manufacture of Li-doped ZnO lean movies by the RF-magnetron sputtering process. How the degree of Li doping influences the optical and electrical properties of ZnO will be talked about. We particularly examined the impact of lithium concentration on the properties of ZnO.

## 2. EXPERIMENTAL WORK

RF-magnetron sputtering strategy was utilized to create zinc oxide coating on glass substrate.

After being treated in acetone and corrosive arrangement ($1/3HCl/2/3HNO_3$), the substrates (18 mm×26 mm×1 mm glass slides) were cleaned with an ultrasonic cleaner. A base radiator is mounted on the water-cooled anode. On the water-cooled anode, a foundation radiator was introduced. In expansion, the substrates were put 65 mm from the target surface and turned 15 times per miniature.

The substrate temperature was measured using a thermocouple and controlled using a feed-back-controlled radiator, which changed from room temperature to 400°C.

To avoid defilement from other gases within the chamber, the chamber was purged to an extreme background weight of 1 Pa earlier in testimony. The restricted amounts of other extra gases were at that point flushed out of the chamber, and the substrate surface was cleaned for 15 minutes with unadulterated argon gas.

After almost five minutes of pre-sputtering to evacuate the surface oxide layer from the target, testimony was started on the ZnO target.

Sputtering was carried out for 120 minutes at a weight of 0.6 Dad in high-quality argon gas (99.999%).

Optical interferon is utilized to determine the thickness of the film. The Shimadzu UV 3100 S spectrometer with double beam and coordinate circle is utilized to assess optical reflectivity and transmittance within the 300–1800 nm wavelength range. Utilizing Swanepoel's method, the refractive file was assessed from the optical information.

The test is warmed in a broiler set to a temperature of 50°C to 80°C, amid which the D.C. resistance and conductivity are recorded.

The A.C. electrical conductivity was tested using an LCR meter (HIOKI 3532-50 LCR Hi TESTER (Japan)).

## 3. RESULTS AND DISCUSSION

### 3.1. Optical Properties

The objective of this study was to determine the impact of Li-doping concentrations 3, 6, and 9 at.% on the optical properties of Li-doped ZnO movies.

Inquire about examining the ghostly absorbance of movies at moo temperatures, understanding sorts of electronic moves, and calculating vitality contrasts and optical constants.

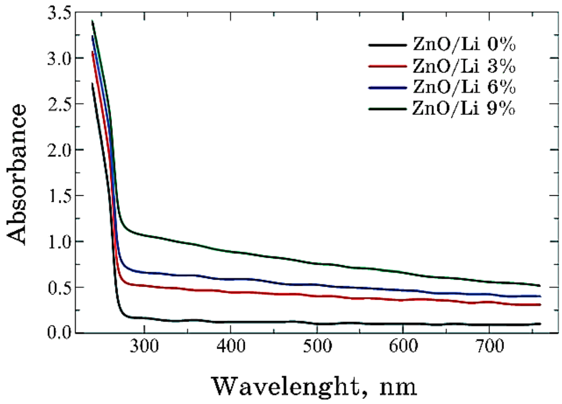


**Fig. 1.** Absorbance spectra of ZnO/Li thin films *versus* the wavelength.

### *3.1.1. Absorbance*

Figure 1 shows the change in absorbance with wavelength of Li-doping concentration 3, 6 and 9 at.% at low temperature. We note that the absorbance of ZnO in the UV region is very high with different Li doping. They are almost equal because the energy of the incident photon of lengths of 400 nm and above is small and not sufficient for electronic transmission. While the energy of ultraviolet waves is high, greater than 3 eV, it is enough to shift one electron from the valence band to the conduction band. This disintegration occurs at a slower rate in the visible and near-infrared ranges, due to the absorption of the ZnO in the ultraviolet region, and the absorption of the composites increases too with the increase in the Li concentration.

### *3.1.2. Transmittance*

Figure 2 presented the spectrum of optical transmittance as a function of the wavelength of the light incident on ZnO by adding different concentration of Li doping. The transmittance decreases as the doping ratios increase. All thin films, including Li, have a high transmittance, greater than 88%, according to the spectra. This is because scattering effects have been reduced, structural homogeneity has improved, and the crystalline state has improved.

### *3.1.3. Absorption Coefficient (A)*

Figure 3 demonstrates that the absorption coefficient ($\alpha$) of elaborated thin films increases as the Li-doping ratios increase, which is

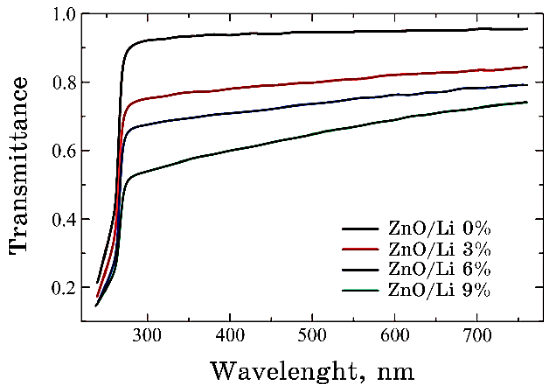


**Fig. 2.** Optical transmittance of the Li–ZnO films *versus* the wavelength.

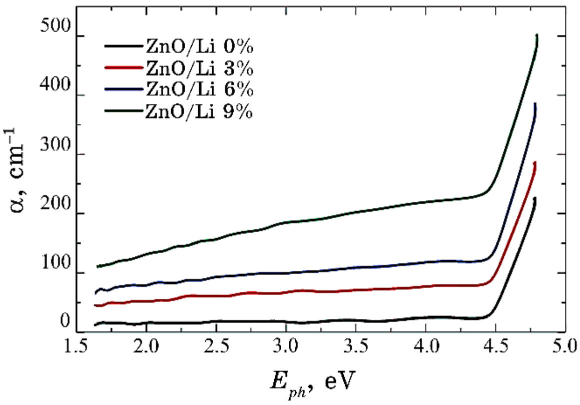


**Fig. 3.** Absorption coefficient as a function of the incident photon energy of the Li-doped ZnO films with various doping ratios.

due to an increase in the number of charge carriers in the films. The result of absorption coefficient (α) for all prepared nanocomposites presented smallest at low energies that could relate to the little possibility of electron transition. Whereas it increases with increasing energy of the incident photon, this indicates that the electron transition has a high probability. The energy of the incident photon is sufficient to interact with atoms. Indirect electronic transitions are extremely likely to occur in accordance with the absorption coefficient (α) values of the prepared films (less than $10^4$ cm$^{-1}$).

### *3.1.4. Optical Energy Gaps Allowed*

The plot of $(h\nu)^{1/r}$ at $r = 2$ *versus* the energy of the photon ($h\nu$) may

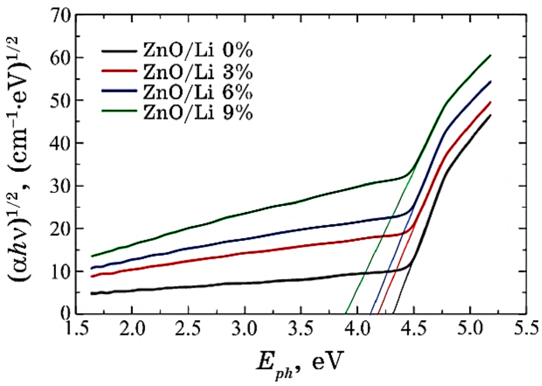


**Fig. 4.** Permissible direct electronic transitions of the Li-doped ZnO films with various doping ratios.

**TABLE 1.** Optical energy gap values allowed for the Li-doped ZnO films.

| Li doping, % | Allowed |
|---|---|
| 0 | 4.25 |
| 3 | 4.1 |
| 6 | 3.29 |
| 9 | 3.7 |

be used to calculate the optical-band energy gap as shown in Fig. 4 based on the absorbance coefficient of Li-doped ZnO thin sheets.

The values, which we obtained, are shown in Table 1, where we notice that the values of the energy gap decrease with the increase in the weight percentages of Li doping. The equivalence package to the local levels and the second transition from the local levels to the delivery package is a result of increasing the proportion of the doping.

### *3.1.5 Refractive Index*

Figure 5 represents the difference in the refractive index ($n$) of the Li-doped ZnO thin films with the emitted photon energy.

The values are increased with the increase in the photon energy, and this indicates that the electromagnetic radiation passes through the Li-doped ZnO films slower in the ultraviolet and visible regions; nevertheless the speed is higher in the visible and near-infrared spectrums.

The refractive index is also increased with the Li doping [in the weight percentages] in relation to the density of the composites.

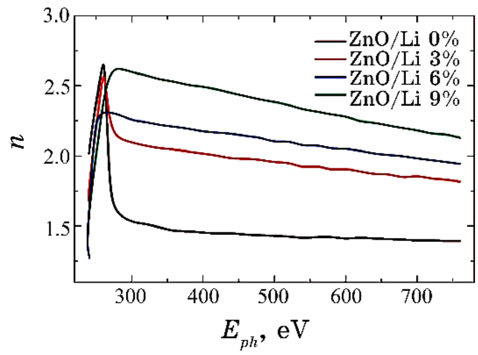


**Fig. 5.** Refractive index of the Li-doped ZnO films with various doping ratios.

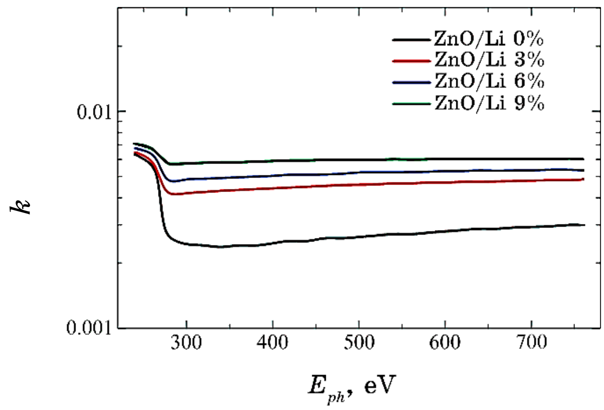


**Fig. 6.** Extinction coefficient of the Li-doped ZnO films with various doping ratios.

### *3.1.6. Extinction Coefficient*

Figure 6 depicts the difference in the coefficient of extinction ($k$) as a function of photon energy for Li-doped ZnO thin film compounds. The coefficient of extinction increases as the concentration of Li doping increases. With an increase in the concentration of Li doping, the deviation increases, so, extinction coefficient ($k$) will increase as a result of the centres of diffusion in the compounds.

### *3.1.7. Dielectric Constant (Real and Imaginary Parts of ( $_r$, $_i$))*

Figures 7 and 8 present the variation of the real ($\varepsilon_r$) and imaginary ($\varepsilon_i$) components of the dielectric constant for pure ZnO and Li-doped

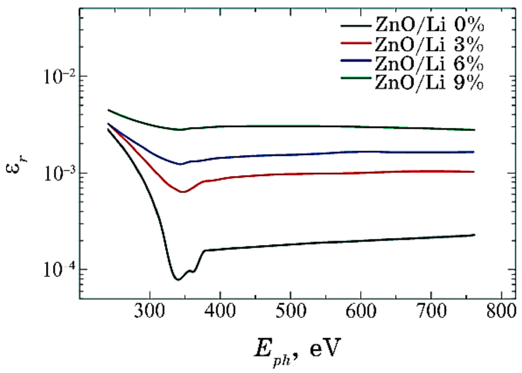


**Fig. 7.** Real dielectric constant of Li-doped ZnO films with various doping ratios.

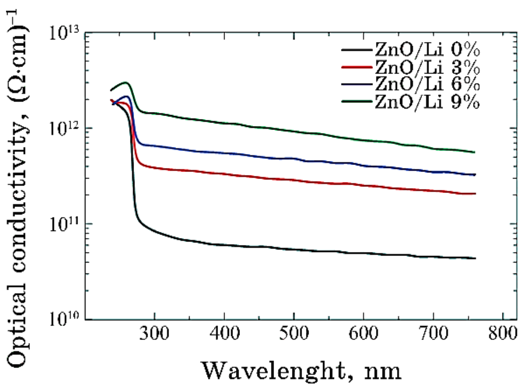


**Fig. 8.** Imaginary dielectric constant of Li-doped ZnO films with various doping ratios.

ZnO films as functions of photon energy ($\varepsilon_r$) presented how much the speed of light was slow down in the material, which is considered a measure of the polarity of a material, whereas ($\varepsilon_i$) demonstrated the dielectric absorb energy by the electric field through the dipole motion. It can be observed that there is an increase in the values of ($\varepsilon_r$) at low photonic energies followed by a clear decrease in the higher energies for all nanocomposite films. A rise in the dielectric constant of Li-doped ZnO films represents a little rise in ZnO internal charges.

### *3.1.8. The Optical Conductivity*

Figure 9 shows how optical conductivity changes as a function of

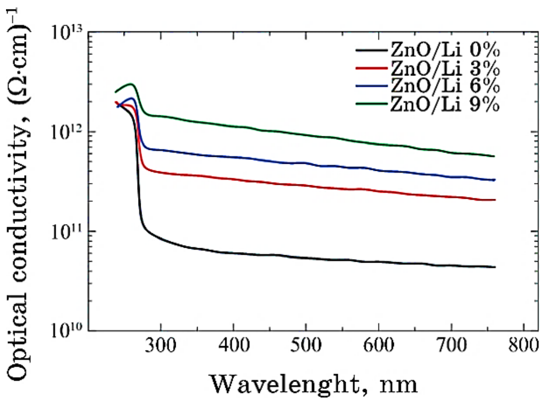


**Fig. 9.** The optical conductivity values *versus* wavelength of Li-doped ZnO films with various doping ratios.

wavelength. The graph demonstrates that, as the wavelength increases, the optical conductivity of all Li-doped ZnO films diminishes. This conductivity-related behaviour is strongly influenced by the radiation wavelength when it hits the nanocomposite samples.

The higher absorption of all Li-doped ZnO films in this region, and thus increased charge transfer excitations, causes an increase in optical conductivity at a low photon wavelength. The samples transmit light in the visible and near-infrared spectrum, according to the optical conductivity spectra.

## 3.2. The Direct Current Electrical Properties of the Li–ZnO Films

### *3.2.1. The Electrical Conductivity of the Li–ZnO Films*

The D.C. electrical conductivity ($\sigma$) is affected by several factors, along with the preparation method and the measurement circumstances.

Figure 10 depicts the temperature ($T$) and Li-doping dependences of $\sigma$ in ZnO films.

The increase in $\sigma$ with Li-doping content could be attributed to the formation of connected networks in the matrix of the thin film. However, since ZnO is a semiconductor, doping it with Li may result in the development of energy levels inside the energy band gap that act as traps for charge carriers that bounce between these levels, boosting DC.

Figure 10 also demonstrates that the DC rises with $T$. This indicates that these films have undergone thermal activation and exhibit semiconductor behaviour.

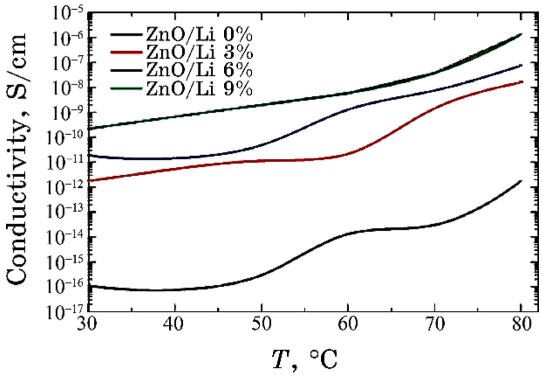


**Fig. 10.** The relationship between D.C. conductivity (σ) and Li-doped ZnO films with various doping ratios.

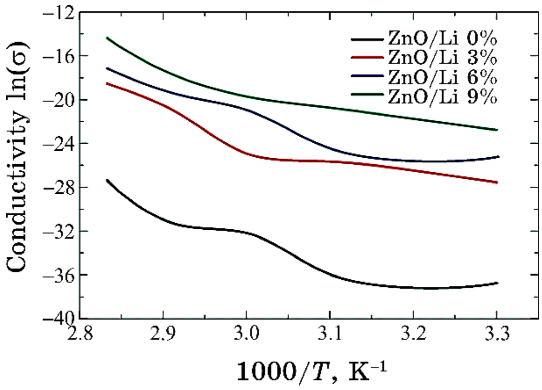


**Fig. 11.** lnσ *versus* ($10^3/T$) of Li-doped ZnO films with various doping ratios.

### *3.2.2. Activation of the Li-Doped ZnO Films*

Figure 11 displays the variation of the absolute temperature $10^3/T$ measured at a temperature range 285–330 K for Li-doped ZnO films as a function of ln.

Electrical activation energy ($E_{ac}$) calculations showed values between 1.576 eV and 1.912 eV, as shown in Table 2.

The presence of free ions in the films is that caused the high electrical activation energy for pure ZnO.

The drop in activation energies with increasing Li doping is related to an increase the energy gap between the local and global levels, which trap charge carriers and are crucial for the transport of charges.

**TABLE 2.** The electrical activation-energy values' experimental results.

| Samples | Activation energy, eV |
|---|---|
| ZnO/Li 0% | 1.912 |
| ZnO/Li 3% | 1.743 |
| ZnO/Li 6% | 1.613 |
| ZnO/Li 9% | 1.576 |

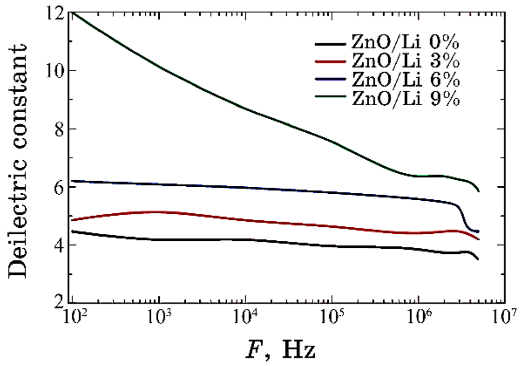


**Fig. 12.** The dependence of dielectric constant of Li-doped ZnO films with various doping ratios and frequency at room temperature.

## 3.3. The Li–ZnO Films' A.C. Electrical Properties

### *3.3.1. The Dielectric Constant*

The value of the dielectric constant indicates a materials' capacity to absorb electricity produced by an applied electric field. Figure 12 illustrates how the dielectric constant varies with the electric field frequency range of $10^2$ to $10^6$ Hz at room temperature. The ratio of 3% Li doping demonstrates the decrease in dielectric constant with rising electric field frequency. This could be as a result of dipole samples' propensity space charges' polarization is reducing as they try to align themselves with the directions of applied electrical fields and with respect to total polarization. The most significant form of polarization is space charge polarization at low frequencies, and as frequency rises, it loses significance.

### *3.3.2. The Dielectric Loss*

The dielectric loss is a measurement of the amount of electrical energy lost in the sample as a result of the applied-field conversion to

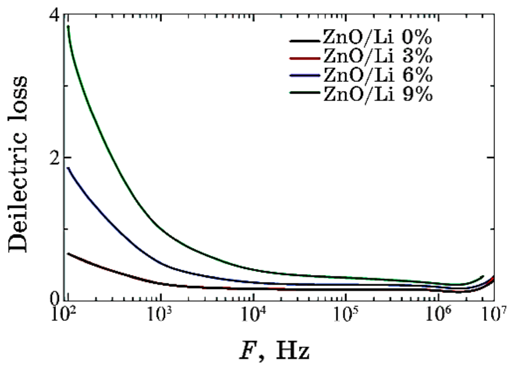


**Fig. 13.** Li-doped ZnO films' dependence on dielectric loss with various doping ratios and frequency at RT.

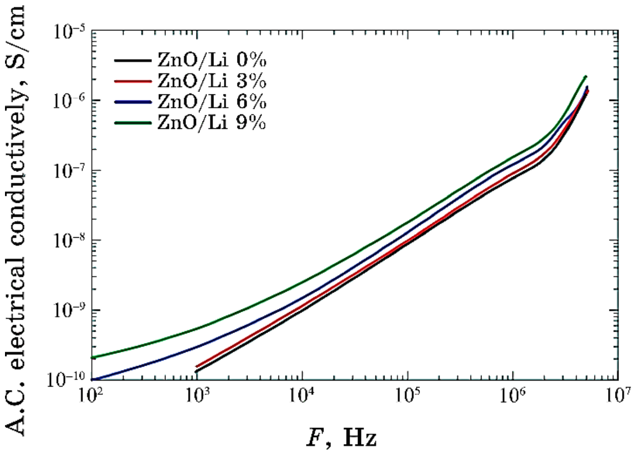


**Fig. 14.** Variation of A.C. electrical conductivity of Li-doped ZnO films with various doping ratios and frequency at room temperature.

thermal energy. The relationship between dielectric loss and the electric field frequency range of $10^2$–$10^6$ Hz. Figure 13 shows thin Li–ZnO films at ambient temperature that thin out as the applied electric-field frequency increases. Reduced space charge polarization's contribution is what causes this.

### *3.3.3. The Electrical Conductivity of A.C.*

As the electric-field frequency increases, the A.C. conductivity increases noticeably. This relationship between the A.C. electrical conductivity and the electric-field frequency range of $10^2$–$10^6$ Hz and both the ZnO and Li doping at room temperature is shown in Fig. 14 for all Li–ZnO thin film samples. This is caused by the hopping motion of charge carriers and space charge polarization, both of which occur at low frequencies. Moreover, as the percentage of Li doping rises, conductivity rises as well. Due to the regular distribution of charge carriers in the Li–ZnO thin films, the increase in space charge as a result of this behaviour is caused by the increase in carriers of charge.

## 4. CONCLUSION

In this work, we examine the impacts of Li doping concentration on the electrical and optical characteristics of Li-doped ZnO films with concentrations 3, 6, and 9 at.%. RF magnetron sputtering was used to create Li-doped ZnO films. The optical characteristics for thin films of (ZnO/Li) revealed that the absorbance, absorption coefficient, and optical conductivity increase as Li concentrations increase, whereas the transmittance and energy band gap decreased as Li concentrations increase. The Li-doped ZnO films' D.C. conductivity at low temperatures was compared to their A.C. electrical characteristics. It is shown that, for all various weight percentages of Li, the dielectric constant and dielectric loss decrease as the electric field frequency rises. All films have single activation energy, according to the electrical characteristics for D.C. measurements, and its value rises with an increase in the percentage of addition.

## REFERENCES


1. J. Wang, H. Pan, X. Xu, H. Jin, W. Ma, S. Xiong, Q. Bao, Z. Tang, and Z. Ma, *ACS Appl. Mater. Interface*, **14**, No. 10: 12450 (2022); https://doi.org/10.1021/acsami.1c22093
2. E. Cheng, S. Huang, D. Chen, R. Huang, Q. Wang, Z. Hu, Y. Jiang, Z. Li, B. Zhao, and Z. Chen, *Acta Crystallogr. C: Struct. Chem.*, **75**, No. 7: 969 (2019); https://doi.org/10.1107/S2053229619008222
3. P. Bhat and S. K. Naveen Kumar, *J. Mater. Sci.: Mater. in Elect.*, **33**, No. 3: 1529 (2022); https://doi.org/10.1007/s10854-021-07664-x
4. K. Singh, H. Kaur, P.K. Sharma, G. Singh, and J. Singh, *Chemosphere*, **313**: 137322 (2023); https://doi.org/10.1016/j.chemosphere.2022.137322
5. G. Voicu, D. Miu, C. D. Ghitulica, S. I. Jinga, A. I. Nicoara, C. Busuioc, and A. M. Holban, *Ceram. Int.*, **46**, No. 3: 3904 (2020); https://doi.org/10.1016/j.ceramint.2019.10.118
6. X. Zhao, K. Nagashima, G. Zhang, T. Hosomi, H. Yoshida, Y. Akihiro, M. Kanai, W. Mizukami, Z. Zhu, T. Takahashi, and M. Suzuki, *Nano Lett.*, **20**, No. 1: 599 (2019); https://doi.org/10.1021/acs.nanolett.9b04367
7. L. Tang, Y. Jia, Z. Zhu, Y. Hua, J. Wu, Z. Zou, and Y. Zhou, *Molecules*, **27**, No. 3: 833 (2022); https://doi.org/10.3390%2Fmolecules27030833

8. M. Kwoka, E. Comini, D. Zappa, and J. Szuber, *Nanomaterials*, **12**, No. 15: 2666 (2022); https://doi.org/10.3390%2Fnano12152666
9. X. Zhan, F. Gao, Q. Zhuang, Y. Zhang, and J. Dang, *ACS Omega*, **7**, No. 10: 8960 (2022); https://doi.org/10.1021%2Facsomega.1c07370
10. S. Nandi, S. Kumar, and A. Misra, *Mater. Adv.*, **2**, No. 21: 6768 (2021); https://doi.org/10.1039/D1MA00670C
11. L. Fan, T. Xiao, C. Zhong, J. Wang, J. Chen, X. Wang, L. Peng, and W. Wu, *Cryst. Eng. Comm.*, **21**, No. 8: 1288 (2019); https://doi.org/10.1039/c8ce01886c
12. S. Y. Tsai, M. H. Hon, and Y. M. Lu, *J. Cryst. Growth*, **326**, No. 1: 85 (2011); https://doi.org/10.1016/j.jcrysgro.2011.01.058
13. S. Ghosh, G. G. Khan, A. Ghosh, S. Varma, and K. Mandal, *Cryst. Eng. Comm.*, **15**, No. 38: 7748 (2013); https://doi.org/10.1039/c3ce40717a
14. Z. Zhang, K. E. Knutsen, T. Merz, A. Y. Kuznetsov, B. G. Svensson, and L. J. Brillson, *J. Phys. D: Appl. Phys.*, **45**, No. 37: 375301 (2012); https://doi.org/10.1088/0022-3727/45/37/375301
15. S. Yu, L. Ding, H. Zheng, C. Xue, L. Chen, and W. Zhang, *Thin Solid Films*, **540**: 146 (2013); https://doi.org/10.1016/j.tsf.2013.05.125
16. M. Rahman, M. Kamruzzaman, J. A. Zapien, R. Afrose, T. K. Anam, M. N. Liton, M. A. Helal, and M. K. Khan, *Mater. Today Commun.*, **33**: 104278 (2022); https://doi.org/10.1016/j.mtcomm.2022.104278
17. K.-H. Wu, L.-Y. Peng, M. Januar, K.-C. Chiu, and K.-C. Liu, *Thin Solid Films*, **570**: 417 (2014); https://doi.org/10.1016/j.tsf.2014.03.062
18. D. Wang, J. Zhou, and G. Liu, *J. Alloys Compd.*, **481**, Nos. 1–2: 802 (2009); https://doi.org/10.1016/j.jallcom.2009.03.111
19. T. T. Wang, M. M. Dai, Y. J. Yan, H. Zhang, and Y. M. Yu, *Appl. Mech. Mater.*, **734**: 796 (2015); https://doi.org/10.4028/www.scientific.net/AMM.734.796